ISOLATION AND CHARACTERISATION OF CELLULOSE FIBRE FROM *PENNISETUM POLYSTACHION* ANDITS APPLICATION IN BIOCOMPOSITES WITH ETHYLENE PROPYLENE DIENE MONOMER RUBBER

KALATHIL T. RAMLATH,[*] PADUPPINGAL SAJNA,[**] POOKKUTH NUSRATH[**] and CHERUMADATHIL RAJESH[**]

[*]*Department of Chemistry, MES Keveeyam College Valanchery, Affiliated to University of Calicut, Kerala 676552, India*
[**]*Department of Chemistry, MES Kalladi College Mannarkkad, Affiliated to University of Calicut, Kerala 678583, India*
✉ *Corresponding author: C. Rajesh, rajeshvlcy@rediffmail.com*

Received August 19, 2023

This article explores an easy and economically viable route for cellulose fibre isolation from the stem of *Pennisetum polystachion* and its utility as reinforcement filler in the polymer matrix for the development of biocomposites. The cellulose fibre was isolated by alkali treatment, followed by chlorine free bleaching using hydrogen peroxide. The SEM and FTIR analyses revealed removal of hemicelluloses and lignin. The X-ray diffraction analysis showed increased crystallinity and the TGA and DTG curves indicated greater thermal stability of the isolated fibre compared to the raw fibre. The cellulose fibre was used as reinforcement in ethylene propylene diene monomer (EPDM) rubber to prepare biocomposites. The cure characteristics and mechanical properties of the composites were investigated. The maximum torque and the mechanical properties varied by the addition of the filler in the matrix. The SEM images of the composites showed good adhesion of the cellulose fiber in the EPDM matrix. The biodegradability of the composites was confirmed by the soil burial test. The test revealed that the percentage degradation in tensile strength increased with filler loading, indicating that the composites are environmentally friendly and biodegradable.

Keywords: *Pennisetum polystachion*, cellulose, biocomposites, cellulose fibre, EPDM rubber

INTRODUCTION

The widespread usage of petroleum products has led to two problems: the depletion of petroleum supplies and the accumulation of plastics in the environment and food chain. The search for an alternative has driven the scientists to bio-based materials that can compete in the markets currently dominated by petroleum-based products. The creation of entirely biodegradable materials to replace petroleum-based products is not a cost-effective alternative. Combining petroleum and bio-based resources to create a product with broad applications would be a more practical solution. Alternatives to glass fibre composites include bio-composites, which are made of bio-polymers or synthetic polymers reinforced with natural fibres.

Scientists are looking for novel polymer composite materials that are sustainable and environmentally benign as a result of rising global temperatures and environmental concerns. Due to their intriguing characteristics, such as low density, light weight, low cost, biodegradability, and abundance, natural fibres can be utilised as reinforcements as an alternative to various synthetic fibres like carbon fibres, Kevlar, glass (mostly S or E glass), *etc*. Natural fibres are being used in a wide range of adaptable ways in the production of natural-based components, including the creation of ropes, vehicle parts, fabrics, minor household applications, as well as aerospace applications. Additionally, they are utilised in natural fibre polymer composites as fillers and reinforcements. Plant fibres have also been touted as a superior substitute feedstock. In any plant, there are three main constituents, with cellulose at the highest composition percentage, followed by hemicelluloses and lignin.[1–5]

Utilising cellulose provides several benefits as it has excellent mechanical properties and is stable, sustainable, biodegradable, and ecologically friendly. At the moment, cellulose that comes from cotton and wood is used in industrial applications. However, wood and cotton are expensive and limited. Because of the shortage of wood resources and the long tree growth cycle, wood is considered as a limited natural resource from the environmental perspective. Hence, recent studies have developed an impressive method for sourcing cellulose from agricultural and food waste, including vegetable trash, durian peel, rubber-wood waste, waste of kenaf-bast fibres *etc*. As a result, cellulosic feedstock from *Pennisetum polystachion* stems is a good choice as it is classified as a second generation source of renewable energy.[6–13]

A thorough understanding of the specific fibre utilised is necessary for the creation of an eco-friendly composite. The qualities of the bonding interaction of the fibre with the matrix and its mechanical, physical, and other properties are among them. Numerous plant fibres, including jute, hemp, flax, coir, kenaf, and flax, have been investigated and used in a variety of applications. Numerous new natural fibres, such as *Prosopis juliflora*, *Tridax procumbens*, *Acacia planifrons*, *Azadirachta indica*, *Ceiba pentandra*, *Heteropogon contortus*, *Epipremnum aureum*, *Calotropis gigantea etc*., have been identified as sources of cellulose fibres that may be used as reinforcement in polymer composites. The development of new fibres that might be used as an essential reinforcement in the polymer matrix phase should consider native plants or widely growing locally in the specific geographic region.

It was found that fibre wettability in the matrix phase contributes to the reinforcement of the composites' mechanical strength properties. With the use of chemical treatment or surface modification, fibre wettability can be attained to a greater extent.[14] The literature contains a number of studies where surface modification is effective in strengthening the fiber–matrix bonding nature to improve the composites' physical, mechanical, and chemical properties. Results indicated that the alkali treatment improved surface roughness and crystallinity, while reducing diameter as a result of the elimination of extra amorphous constituents.[15] Similar results were seen for *Tridax procumbens*, where NaOH treatment improved the physical, mechanical, and chemical characteristics of the fibre.[5] From the literature results illustrated above, it can be concluded that chemical treatment removes the amorphous contents, increasing the surface wettability and leading to firm bonding with the matrix when the fibre is used in composites.

Various methods for the isolation of cellulose, such as chemical, mechanical and biological, have been described.[16–21] The objective of such treatments is to break down the biomass polymers, reduce hemicelluloses and lignin content, as well as improve the cellulose content.[22] The chemical methods are widely used as they are easy, cheap and efficient. The alkali based treatment is more appropriate for lignocellulosic biomass.[23] Alkaline hydrogen peroxide bleaching treatment has a lower environmental impact than chlorine containing bleaching agents, like sodium chlorites and hypochlorites.[24,25] The alkali treatment removes some amount of lignin, hemicelluloses, extractives, wax and oil. The bleaching process leads to oxidation and solubilization of chromophoric groups of the residual lignin and natural dyes in the fibre.[26]

Pennisetum polystachion, commonly called as mission grass, a widespread species belonging to the family of Poaceae. It is a vigorous perennial grass, 1-2 m in height, with long leaves – 5-50 cm – and yellow brown flowers with seeds, usually with a few branches. The inflorescence is a very dense, narrow panicle containing fascicles of spikelets interspersed with bristles. There are three kinds of bristle, and some species have all three, while others do not. Some bristles are coated in hairs, sometimes long, showy, plume like hairs that inspired the genus name, the Latin "penna" (feather) and "seta" (bristle). It thrives in warmer, drier areas and threatens many native species, with which it competes very effectively as an invasive species. It also tends to increase the risk of intense wildfires, to which it is well adapted, thus posing a further threat to certain native species. As currently envisioned, *Pennisetum* is a genus of 80 to 140 species. The various species are native to Africa, Asia, Australia, and Latin America, with some of them widely naturalized in Europe and North America. It is a vigorous natural invader seen as spreading along the road sides, agricultural fields and natural habitats in all districts of the southern Indian state of Kerala.

The ethylene–propylene–diene monomer (EPDM) rubber is an amorphous compound and is increasingly demanded in many fields due to its

aging resistance to heat, ozone, chemicals and solvents, as well as its excellent mechanical, electrical properties and processing abilities with reinforcing agents and plasticizers. The EPDM compound is often reinforced with the various particles (such as carbon black, silica, glass beads, *etc*.) because of its low stiffness and low tensile strength (*i.e*., 6.8 and 12.5 MPa, respectively). When the fillers are incorporated into the matrix material to produce composites, not only the properties of the fillers and of the matrix, but also the interphase plays an important role in the development of the composites. These composites find use in a wide range of applications, such as construction, aerospace and automotive industries.[27–36]

The possibility of using *P. polystachion* for the extraction of cellulose has not been reported yet, to the best of our knowledge. Therefore, in this work, the cellulose fibre was isolated from *P. polystachion* grass and its composition, morphology, crystallinity and thermal properties were studied. The feasibility of the extracted cellulose as reinforcement in polymer bio-composites was assessed in EPDM rubber, using dicumyl peroxide as vulcanizing agent. The cure characteristics and mechanical properties of the composites were studied. Further, the biodegradability of the composites was analysed by soil burial tests.

EXPERIMENTAL

Materials

The grass *Pennisetum polystachion* was collected from nearby fields in Palakkad district, Kerala. Chemicals, solvents and reagents, such as NaOH and H_2O_2, were supplied by Merck India Ltd. EPDM rubber and dicumyl peroxide (DCP) were supplied by Joefex Chemicals, Kottayam, Kerala, India.

Methods

Sample preparation

The root, flowers and leaves of *P. polystachion* grass were removed and the stem was cleaned well and was cut into very small pieces. It was then dried under sunlight for about ten days, ground and the weight of the dried sample was noted.

Determination of chemical composition of fibre

The major chemical constituents – lignin, hemicelluloses and cellulose – were determined as per ASTM standard methods. Firstly, the moisture content was determined as per ASTM D-1348 method. The extractives were determined by ASTM D 1107-96. Thus, the feedstock was subjected to a Soxhlet extraction procedure using a mixture of ethanol and toluene (2:1) for the extraction of any inorganic materials and non-structural sugars from the samples, such as chlorophyll, waxes, sterols, and lipids. The lignin content was then determined by ASTM D 1106-96 method. The holocellulose was determined by the method described by Wise *et al*.,[37] the α-cellulose content was subsequently determined by ASTM D 1103-60 and the hemicelluloses content was estimated as the difference between holocellulose and α-cellulose contents.

Cellulose extraction

The extraction of cellulose from *P. polystachion* requires alkali treatments and bleaching. In all these treatments, a liquor ratio of 1:30 (g/mL) was used. The alkali and acid pre-treated fibre was treated with NaOH of different concentrations at 50 °C for 2 hours. Then, bleaching was done by treating the alkali treated fibre with an alkaline solution of H_2O_2 at 50 °C under constant stirring for 2 hours. The procedure was repeated until a white mass of cellulose was obtained.

Preparation of composites

The formulations of mixes for the different series of composites are given in Table 1. The fabrication was carried out by using a laboratory two-roll mixing mill. Initially, EPDM was masticated on the mill for 2 min, followed by the addition of the ingredients. The vulcanizing agent used was dicumyl peroxide (DCP). The nip gap, mill roll speed ratio, total mixing time and the number of passes were kept the same for all the mixes. The samples were milled for sufficient time to disperse the filler in the matrix. Care was taken to ensure temperature not to become too high, so as to avoid crosslinking during mixing and this was achieved by water circulation.

Vulcanization of composites

Different composite mixes were vulcanized for the respective cure time obtained from a rheograph at 150 °C, using a hydraulic press with electrically heated plates (150 mm x 150 mm x 2 mm). The sheets obtained with 2 mm thickness were moulded longitudinally along the fibre direction and were conditioned by keeping in a cold dark place as per the ASTM D 412 test method. From the sheet, the sample specimens were cut in order to study their mechanical properties.

Characterization of cellulose fibre and composites

FTIR spectroscopy

A Fourier transform infrared spectrophotometer was used to analyze the constituents and the functional groups in the fibre, alkali treated fibre and bleached cellulose fibre. The test can also be used to monitor the changes taking place to the constituents and functional groups during the isolation process through alkali

treatment and bleaching. The removal of lignin and hemicelluloses can be verified from the FTIR data.

Thermogravimetric analysis (TGA)

The thermal behaviour of the grass fibre, bleached fibre and EPDM cellulose fibre composites was assessed using an STA 8000 thermal analyzer. The sample, weighing in the range of 3-6 mg, was heated in a furnace in a flowing nitrogen atmosphere, at a flow rate of 20 mL/min to prevent unwanted oxidation. The sample was heated from 30 ℃ to 600 ℃, at a heating rate of 10 ℃/min. The thermal stability, temperature of different weight loss and the residual weight can be obtained from the TG curves.

Table 1
Composite formulations (phr*)

Components	Sample						
	A (gum)	B	C	D	E	F	G
EPDM	100	100	100	100	100	100	100
Cellulose fibre	-	5	10	15	20	25	30
DCP**	1.5	1.5	1.5	1.5	1.5	1.5	1.5

*Parts per hundred rubber, **Dicumyl peroxide

X-ray diffraction analysis (XRD)

X-ray diffraction analysis (XRD) was performed to investigate the crystalline features of raw fibre and isolated cellulose fibre and the diffractograms were obtained. The X-ray diffraction patterns of the samples were recorded using an XPERT-3 diffractometer system. The data were generated in the 2θ range from 0^0 to 100^0 with Cu Kα radiation (λ = 1.54 Å). Segal's method was used to determine the crystallinity index, CrI. Segal's method is an empirical method to determine the relative crystallinity. The crystallinity was calculated by the formula:[38]

$$CrI = \frac{(I\ max - I\ min)}{I\ max} * 100 \quad (1)$$

where I_{max} is the highest intensity at 2θ and I_{min} is the lowest intensity.

SEM analysis

SEM analysis was carried out to study the morphological changes occurring in the cellulose fibre after the treatments and the morphology of the fracture surface of the composites. The scanning images of raw fibre, treated cellulose fibre and composites were obtained using a JEOL JSM-6390 scanning electron microscope, with an accelerating voltage of 15 kV, at magnification of x100, x250, x500, x1500 and x3000.

Mechanical properties

Tensile strength, Young's modulus and elongation at break were determined using a Shimadzu Universal Testing Machine (UTM), at a crosshead speed of 500 mm/min according to ASTM D 412-68 method. The thickness of the narrow portion of the sample was measured at three different points, using a thickness gauge, and the average value was taken. The specimens cut along the grain direction were placed vertically in the grips of the UTM having the gauge length kept at 40 mm. On starting the test, the grip pulls out, the specimen elongates and then it gets broken. The tensile properties indicate the ability of the composites to withstand the pulling force and the limit to which the material can be stretched before breaking. Dumb bell-shaped standard samples were used for the measurement of tensile properties. The tensile properties were recorded in the machine. The tensile strength and elongation at break were calculated by Equations (2) and (3), respectively:

$$Tensile\ strength = \frac{Force(Load)\ (N)}{Area\ of\ cross\ section\ (mm^2)} \quad (2)$$

$$Elongation\ at\ break = \frac{Change\ in\ length}{Original\ length} \quad (3)$$

RESULTS AND DISCUSSION

Composition of raw material

The percentage composition of the grass sample was determined and is given in Table 2. Also, for comparison, the composition of some non-wood, cereal straws and perennial grasses is tabulated in Table 3.[39,40] The results show that this fast-growing perennial grass has appreciable cellulose content and, hence, this raw material can be used as a potential source for cellulose extraction.

Extraction of cellulose fibres

The cellulose fibres were extracted by the alkali treatment, followed by bleaching. The dried and ground grass sample had a yellow colour. Upon the alkali treatment, the disintegration of the fibres was observed, and the colour turned to brown, indicating only partial removal of lignin, hemicelluloses and other components. The bleaching treatment results in the disappearance

of the brown colour, yielding more fragmented white fibrils, a visual indication of the removal of the cementing materials. The bonds, such as ester or ether linkages, between lignin units or lignin with other carbohydrate units may be broken up by the alkali and bleaching treatments, leading to the partial defibrillation of the grass fibres.[41,42] Figure 1 shows photographs of *Pennisetum polystachion* grass in the field (Fig. 1a), untreated fibre (Fig. 1b), alkali treated fibre (Fig. 1c), and cellulose fibre (Fig. 1d).

Table 2
Percentage composition (w/w %) of *Pennisetum polystachion* grass

Components	% Weight
Moisture	4.6±0.3
Extractives	3.6±0.2
Holocellulose	72.0±2.1
Hemicelluloses	27.6±0.3
Lignin	21.3±1.4
Cellulose	44.5±1.5

Table 3
Comparison of cellulose content and % composition (w/w) for some cellulose-based fibres

Fibre source	Cellulose, %	Hemicelluloses, %	Lignin, %
Bagasse	38.9	22.4	25.1
Banana	34.5	25.6	12.0
Cotton stalks	58.5	14.4	21.4
Rice straw	33.0	26.0	7.0
Peanut shell	22.1	12.1	35.2
Sago seed shell	36.5	22.5	23.6
P. polystachion	44.5	27.6	21.3

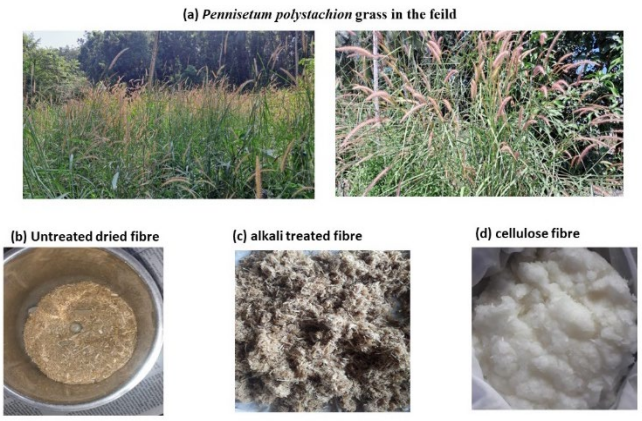

Figure 1: Photographs of (a) *Pennisetum polystachion* grass in the field, (b) untreated fibre, (c) alkali treated fibre and (d) cellulose fibre

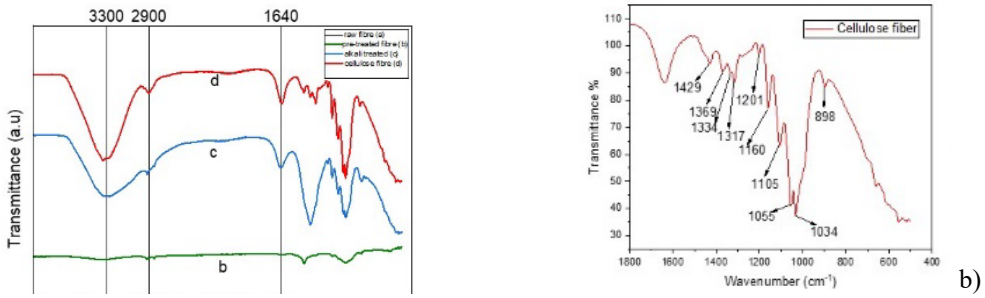

b)

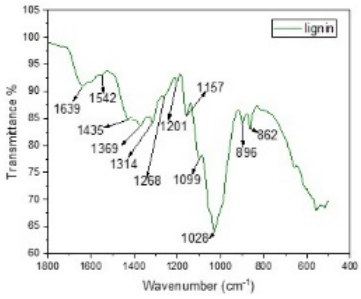

c)

Figure 2: (a) FTIR spectra of raw fibre, pretreated fibre, alkali treated fibre and cellulose fibre; (b) the finger print region of cellulose; and (c) the finger print region of lignin

Characterization

FTIR spectroscopy

FTIR spectroscopy was employed to examine the changes in chemical composition of the grass fibre occurring after the alkali treatment and bleaching during the cellulose isolation process, and to confirm the nature of the obtained sample and the removal of lignin. The FTIR spectra of raw fibre, pretreated fibre, alkali treated fibre and isolated cellulose fibre are shown in Figure 2 (a).

As may be noted, the spectra of the alkali treated fibre and isolated cellulose fibre are well defined, compared to that of the untreated fibre. Also, the intensity of the peaks was noted to increase due to chemical treatments. The broad band at around 3000-4000 cm^{-1} is due to the -OH groups of cellulose, hemicelluloses and lignin. This band covers the inter- and intramolecular hydrogen bonded O-H stretching vibrations.[43] The alkali treated cellulose and isolated cellulose exhibit these peaks with high intensity, which indicates higher percentage of exposed -OH groups, compared to the untreated fibre.[44] The band at 2800-3000 cm^{-1} is attributed to the C-H bond. The peaks at 2920 cm^{-1} and 2850 cm^{-1} indicate stretching vibrations of methyl and methylene groups of cellulose, hemicelluloses and lignin.[45] The peak appearing at 1640 cm^{-1} can be attributed to stretching O-H vibrations of absorbed water molecules.[46] The broad peak at 3331 cm^{-1} is the characteristic frequency of the stretching vibrations of polysaccharides.[47,48]

The finger print region of cellulose from the FTIR spectrum of the isolated cellulose is given in Figure 2 (b). The typical IR peaks assigned to cellulose are in the range of 1630-900 cm^{-1}.[47,48] The absorption frequencies at 1429, 1369, 1334, 1317, 1160, 1105, 1055, 1034 and 897 cm^{-1} are typical bands for polysaccharides. The frequencies at 1428, 1369, 1334, 1034 and 897 cm^{-1} are assigned to the stretching and bending vibrations of CH_2, CH, OH and C-O bonds in cellulose.[49,50] The peak at 1429 cm^{-1} is associated with the crystalline structure of cellulose, while the peak at 897 cm^{-1} – with the amorphous structure.[51] The bands appearing at 1425, 1372, 1425, 1372, 1320, 1160, 1031 and 897 cm^{-1} can be due to CH_2 bending vibrations, C-O-C pyranose ring skeletal vibrations, C-O stretching and C-H rocking vibrations of cellulose.[52] The peaks at 1429 and 1369 cm^{-1} correspond to CH_2 stretching and C-H bending vibrations, respectively. The peak at 1317 cm^{-1} corresponds to the bending vibrations of the C-O group present in crystalline cellulose. The peak at 1034 cm^{-1} is due to C-O stretching.[40,53] The bands appearing at 1317 cm^{-1} can be attributed to CH_2 wagging vibration in cellulose. Also, the peak at 1160 cm^{-1} can be related to C-O-C asymmetric stretching vibration of cellulose.[44] The absorption bands from 1110-999 cm^{-1} represent C-O-C pyranose ring skeletal vibrations of cellulose. Also, the peak at 898 cm^{-1} corresponds to C-H rocking vibrations, representing the typical cellulose structure of β-glycosidic linkages. These peaks became prominent after the chemical treatments, indicating the removal of hemicelluloses and lignin.[45,54,55]

The finger print region of lignin is presented in Figure 2 (c). Lignin acts as a binder or glue between cellulose fibres in the raw material. It has a complex three-dimensional structure. Structural components consist in phenyl, methyl and methylene groups and, hence, the spectrum obtained shows bands due to these subunits. The peak at 1435 cm^{-1} is due to the stretching vibrations of the $O\text{-}CH_3$ group and that at 1268 cm^{-1} is due to C-O stretching of aryl groups.[56] The peak at 862 cm^{-1} is due to the C-H bond of aromatic hydrogen in lignin. The bands appearing at 1600, 1514 and 1455 cm^{-1} correspond to C-H deformation in methyl, methylene and methoxy groups of lignin. The absorption at 1235 cm^{-1} is

attributed to the axial asymmetric stretch of C-O of the corresponding groups in lignin.[52]

Thermogravimetric analysis (TGA)

Thermogravimetric analysis (TGA) curves of raw fibre and isolated cellulose fibre are presented in Figure 3 (a). The thermograms demonstrate that thermal decomposition takes place in four stages in the ranges 22-138 °C, 173-365 °C, 299-428 °C and 173-649 °C, corresponding to the evaporation of moisture, and degradation of hemicelluloses, cellulose and lignin, respectively. Both curves show decomposition at the onset temperature of 22-138 °C, due to evaporation of water and volatile extractives.[57] The second stage of weight loss occurred at 173-365 °C, and was attributed to the degradation of portions of lignin and hemicelluloses.[58] Hemicelluloses decompose into CO, CO_2, and hydrocarbons at a lower temperature than lignin and cellulose.[56] This is due to the fact that hemicelluloses consist of sugars, such as glucose, galactose, mannose and xylose, having an amorphous structure. The third stage of weight loss at 299-427.5 °C is attributed to cellulose decomposition.[59] At this stage, a major mass reduction of approximately 60% occurred due to the elimination of cellulosic components. The fourth stage, at 173-649 °C, is due to the degradation of lignin and wax.[60] The lignin gives strength and rigidity to the plant cell wall, and the presence of the phenyl ring in the complex polymeric material of lignin make it difficult to degrade. Lignin serves as a binding agent in plant cell tissues. Hence, lignin degradation showed no maximum weight loss rate throughout the temperature range.

The TG curve of the raw fibre shows a wide degradation range at 30-600 °C. The decomposition of the cellulose fibre mainly occurs in the range of 30-380 °C, which is due to the removal of moisture and the degradation of cellulosic components.

From the thermograms of both the raw fibre and the cellulose fibre, it is clear that the first stage of decomposition is due to a decrease in the moisture content and volatile extractives, which is lower for the cellulose fibre, compared to the raw fiber. Low moisture content is preferred for the manufacture of polymer composites due to their lesser ability to retain water molecules. The moisture content is a significant parameter, as it also affects the physical properties and dimension of the fibre.[61] It influences the porosity, dimensional stability, tensile strength and swelling properties of natural fibre reinforced composites.[43,62]

The TG curve of the cellulose fibre is well defined, indicating an ordered or more crystalline structure. The decomposition temperature of the cellulose fibre at 254 °C is higher than that for raw fibre, which is at 212 °C. Also, the final residual mass is lower than that for raw fibre, indicating the removal of non-cellulosic components. The decomposition of cellulose fibre starts with the depolymerization and dehydration process to yield the glucose units, which then undergo breakdown and charring to get gaseous products. This indicates removal of amorphous hemicelluloses and lignin.[63]

The DTG thermograms, derivative of the thermogravimetric curves, are also presented for the raw fibre and cellulose fibre in Figure 3 (b). The curve shows that the DTG peaks for the raw fibre and the cellulose fibre are around 295 and 355 °C, respectively. The higher DTG_{max} for the cellulose fibre indicates an enhancement of thermal properties and thermal stability for the cellulose fibre, compared to the raw fibre. This is due to the removal of lignin and other non-cellulosic components from the fibre and due to the higher crystallinity.[45,59,64] This enhanced thermal property makes the obtained cellulose a better reinforcement material in biocomposites.

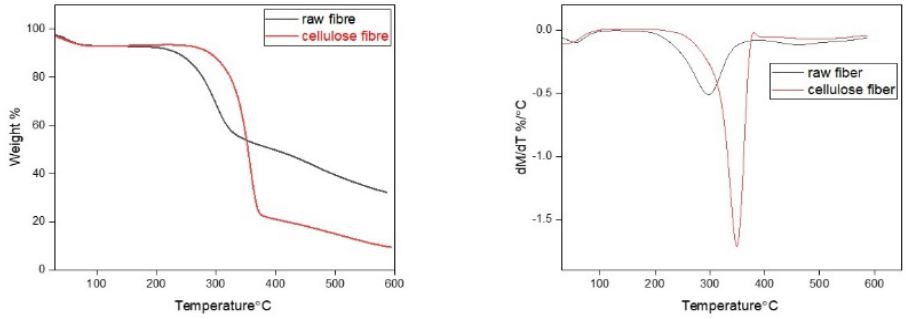

a) b)

Figure 3: (a) TGA and (b) DTG curves of raw fibre and cellulose fibre

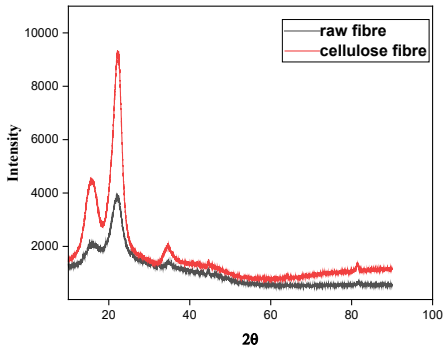

Figure 4: XRD patterns of raw fibre and cellulose fibre

X-ray diffraction analysis (XRD)

The XRD results for the raw grass fibre and cellulose fibre are presented in Figure 4. From the figure, it is clear that the peaks in the X-ray pattern of raw fibre is not well defined, but the peaks of isolated cellulose are sharp. The peaks can be observed at 2θ of 22.2^0 (sharp and intense), 34.5^0 (small) and a shoulder peak at 15.6^0 (broad), which demonstrate a typical cellulose 1 structure. The peak at 15.6^0 corresponds to the (1-1 0) and (1 1 0) of cellulose I. Also, the peaks at 22.2^0 and 34.5^0 represent (2 0 0) and (0 0 4) crystallographic planes of cellulose I.

The degree of crystallinity, CrI values were determined from the X-ray diffraction patterns. The results demonstrated that the CrI increased from the raw plant fibre to the isolated cellulose fibre. The CrI values for the raw grass fibre and cellulose fibre were 43.86% and 51.30%, respectively. The higher value for CrI in cellulose fibre is due to the removal of lignin, hemicelluloses *etc*. that were attached to the cellulose.[43]

Cure characteristics of composites

The rheometric curves of the different cellulose fibre/EPDM composites are given in Figure 5. Cure characteristics, such as maximum torque (M_H), minimum torque (M_L), cure extend (M_H-M_L), cure time (t_{90}) and scorch time (t_{10}), of the EPDM-cellulose fibre composites were obtained from the rheographs and are presented in Table 4.

Cure time t_{90} is the time taken to achieve 90% of crosslinking or 90% of maximum torque, and scorch time t_{10} is the time taken for attaining 10% of the maximum torque. The cellulose fibre composites have longer cure time due to the better reinforcing interaction with the polymer matrix.[65] However, there is not very much difference in the cure time upon the addition of fillers. This indicates that the rubber matrix phase plays a more significant role in natural fibre polymer composites.[66] Minimum torque (M_L) is the measure of stiffness in the unvulcanised state. Vulcanization of rubber results in an increase in torque. Maximum torque (M_H) is a measure of stiffness, reinforcement or crosslink density of the vulcanised mixes. It is recorded after the completion of curing. It can be seen that, for all mixes, the torque initially decreases, then increases and finally levels off. The initial decrease in torque to a minimum value is due to the softening of the matrix, followed by an increase, which is due to an increase in crosslinking, and a levelling off, which is an indication of maximum crosslinking.

From Table 4, it is found that the addition of the cellulose fibre to the matrix increases maximum torque. As more fibre is dispersed into the matrix, the mobility of the polymer chains of the matrix is restricted, resulting in stiffness and hardness of the composites. The treated fibre reinforcement leads to higher torque values, as it provides better surface for adhesion to the polymer matrix, resulting in enhanced reinforcement for the matrix.[65]

During vulcanization, the interaction of curing additives takes place in the first stage, called induction period or scorch time. In the next stage, further reactions between the additives, curing agent and matrix functional groups take place, with the formation of crosslinks. The induction period and the subsequent curing depend on the nature of the rubber, the composition of the curing system and the formulations of the composites. Peroxide vulcanization is a radical process, involving the formation of carbon-carbon linkages.[67–69]

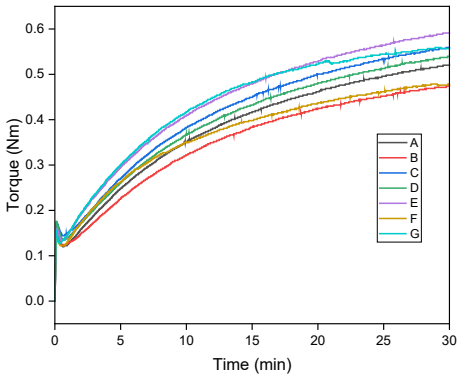

Figure 5: Effect of filler loading on maximum torque of cellulose fibre/EPDM composites

Table 4
Cure characteristics of different cellulose fibre/EPDM composites

Sample code	Fibre loading (phr)	Scorch time (min)	Cure time (min)	M_H (Nm)	M_L (Nm)	Δm (Nm)
A	0	8	22	0.50	0.10	0.40
B	5	2	23	0.47	0.10	0.37
C	10	2	23	0.56	0.13	0.43
D	15	1	23	0.54	0.12	0.42
E	20	1	22	0.59	0.11	0.48
F	25	1	20	0.49	0.11	0.38
G	30	1	20	0.61	0.12	0.49

SEM analysis

Figure 6 (a and b) shows the SEM images of untreated fibre and isolated cellulose fibre, respectively. The SEM micrographs reveal that morphological changes took place during the isolation process. The diameter of the cellulose fibre is lower than that of the untreated fibre, and it is expected that a 12-45% reduction occurred due to the alkali and bleaching treatments during the isolation of cellulose.[44,70] These micrographs demonstrate that the raw fibre surfaces are covered with wax, impurities and other fatty substances.[71] The alkali and bleaching treatment processes can break up the lignocellulosic fibre, solubilizing lignin and hemicelluloses, yielding cellulose fibre with higher porosity and surface area. Hemicelluloses act as compatibilizer between cellulose and lignin, which acts as binder. These are removed during the isolation process, as evident from the SEM image of the cellulose fibre. The micrograph shows aggregated and non-aggregated fibres, with coalesced boundaries, having rougher surface. This rough surface allows better mechanical interlocking and binding reaction, thereby increasing the filler–matrix interaction in composites.

The morphology of the fractured surfaces of the composites was also analysed by SEM. The micrographs of the gum sample and the composite with 25 phr filler loading are shown in Figure 6 (c) and (d), respectively. The gum sample shows a smooth uniform surface. The cellulose fibres and EPDM matrix are different kinds of materials, having different properties. From the images, it can be observed that the fibres are distributed in the matrix possibly by some physical interaction.

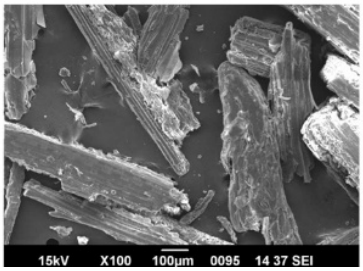

a)

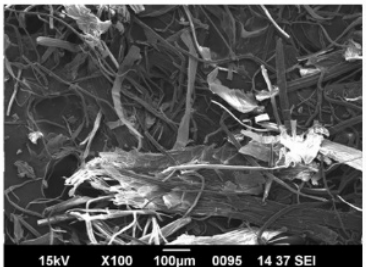

b)

c) d)

Figure 6: SEM images of (a) untreated fibre, (b) cellulose fibre, (c) gum composite, and (d) cellulose fibre/EPDM composite

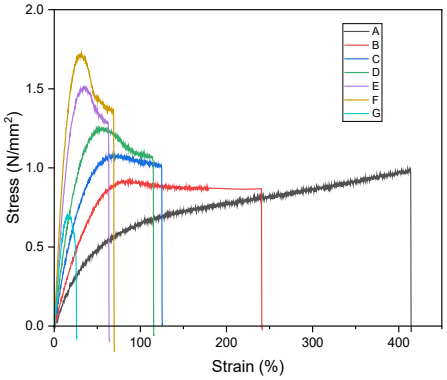

Figure 7: Effect of filler loading on stress-strain curves of cellulose fibre/EPDM composites

Mechanical properties

The stress-strain curves of the different cellulose fibre/EPDM composites having different filler loading are shown in Figure 7. It can be noted that the slope of the initial linear part of the curve increases, as the cellulose fibre loading increases, clearly indicating the reinforcement of the filler in the rubber matrix. The mechanical properties – tensile strength, elongation at break, Young's modulus and tear strength – of EPDM composites containing cellulose fibres at different loading as fillers in the presence of dicumyl peroxide as curing agent are shown in Figure 8. The parameters are found to be affected by the percentage of fibre and are also given in Table 5.

The increase in Young's modulus with the rise in the filler loading is due to higher fibre–matrix interaction, and a peak in the graph is observed corresponding to the 25 phr fibre loading, indicating maximum bonding interaction and stiffness at this point. However, further increase in cellulose fibre loading decreases the values, because the continuity of the matrix phase was disturbed.

The tensile strength is found to increase with the addition of cellulose fibre to the EPDM matrix. The adhesion between the matrix and the filler is enhanced, causing more effective stress transfer from the EPDM rubber matrix to the cellulose fibre filler. Generally, the tensile strength drops down at lower fibre loading and then increases. The tensile strength is found to increase up to the filler loading of 25 phr and then after decreases, signifying that the strength of the composite increases only up to 25 phr and further increase of filler loading causes agglomeration of the filler, leading to a discontinuous fibre matrix phase. This results in less effective stress transfer from the matrix to the filler.

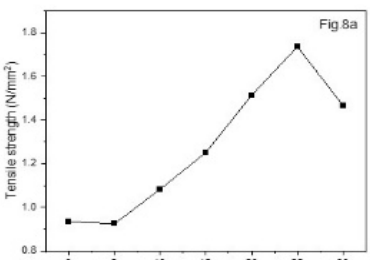

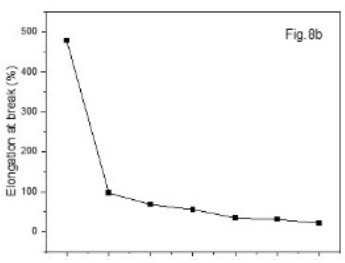

a) b)

c) d)

Figure 8: Effect filler loading on (a) tensile strength, (b) elongation at break, (c) Young's modulus, and (d) tear strength of cellulose fibre/EPDM composite

Table 5
Effect of fibre loading on mechanical properties of EPDM composites

Sample code	Tensile strength (N/mm^2)	Elongation at break (%)	Young's modulus	Tear strength (N/mm)
A	0.93449	477.845	0.01352	5.52098
B	0.92430	96.8037	0.02026	10.2368
C	1.08291	68.0536	0.03274	14.2545
D	1.25168	55.5536	0.04484	15.4398
E	1.51360	34.7204	0.07980	16.9253
F	1.73630	30.7620	0.10457	19.049
G	1.22907	21.3871	0.06442	10.3081

The elongation at break is found to decrease abruptly at lower filler loading and then declines gradually. This suggests that, along with the increase of strength and stiffness of the composites, the brittleness also increases, causing reduction in elongation at break with the addition of cellulose fibres to the polymer matrix. The elongation at break can be correlated with the crosslink density and hence the extent of reinforcement. The higher the crosslink density of the composites, the lower the elasticity and mobility of the polymer chains, and the lower the elongation at break will be.[72]

Biodegradability studies

Soil burial tests are used to assess the biodegradability and degradation of materials when exposed to the soil environment. The test provides valuable information on the long-term behavior and degradation of biocomposites in the soil environment, helping to assess their environmental impact and suitability for specific applications. The tensile strength of the dumbbell shaped specimens was measured[73] before and after the soil burial test and was compared. It has been noted that, increasing the filler loading causes a drop in tensile strength and thus results showed higher biodegradation. The percentage decrease in tensile strength of the composites with different filler loading is shown in Figure 9. The deterioration of the composites' mechanical characteristics is an indicator of the biodegradation behaviour by the soil microorganisms.

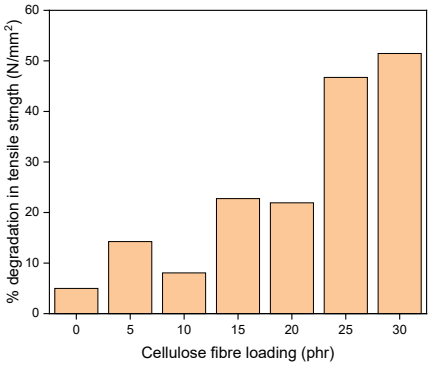

Figure 9: Percentage decrease in tensile strength of cellulose fibre/EPDM composites after soil burial test

CONCLUSION

The main objective of this study was to extract the cellulose fibre from *Pennisetum polystachion* grass and to explore its application potential as reinforcement filler in polymer biocomposites. The composition of the grass fibre was determined by chemical analysis, which revealed the percentages of moisture content, extractives, α-cellulose, hemicelluloses and lignin. The cellulose isolation was carried out by a two-step process of alkali treatment and bleaching, which was performed by the more environmentally friendly chlorine-free hydrogen peroxide method. The alkali treatment resulted in the solubilization of most of the lignin and hemicelluloses, as evident from the FTIR spectra. Further, the bleaching treatment performed the removal of most of the lignin and hemicelluloses, as evident from the visual observation – whitening of the fibre –, which was supported by FTIR spectroscopy showing higher intensity of characteristic cellulose peaks. The XRD data revealed increased crystallinity of the isolated cellulose, compared to the raw fibre, and TG analysis showed higher thermal stability of the extracted cellulose fibre. These findings confirmed the removal of amorphous hemicelluloses and lignin components. The SEM images of the isolated fibres illustrated more porous and rougher aggregated and non-aggregated fibrils, having higher surface area due to the removal of the binder and compatibilizer elements – lignin and hemicelluloses, respectively. All these show that cellulose fibres have been successfully isolated from the *P. polystachion* grass. Thus, the rougher and more crystalline nature of the isolated cellulose fibres enables better binding and mechanical interlocking with the polymer matrix. Hence, this study supports the feasibility of utilising *P. polystachion* grass cellulose fibres as reinforcing material in polymer composites.

The cure characteristics and mechanical properties, such as tensile strength and Young's modulus of the cellulose fibre/EPDM composites were studied. The addition of the fibre caused an increase of maximum torque values and cure time, as well as an enhancement in mechanical properties. These results indicate good interfacial adhesion between the cellulose fibre and the EPDM matrix. The SEM images confirmed uniform distribution of the filler in the matrix, further supporting the reinforcement of the cellulose fibre.

Hence, this investigation is a search for an economic route for the utilization of naturally abundant *P. polystachion* grass, a fast invader of cultivated lands and wastelands, for the isolation of cellulose and its application as reinforcing agent in an EPDM rubber matrix. Further study will be focussed on the development of biocomposites with improved bonding interaction between the fibre and the matrix to achieve higher dispersion of the cellulose fibre in the rubber matrix for versatile product applications.

ACKNOWLEDGEMENTS: This work was supported by FIST funding of the Department of Science and Technology, Govt. of India [SR/FST/College-191/2014].

REFERENCES

[1] S. Siengchin, J. Parameswaranpillai, M. Jawaid, C.I. Pruncu and A. Khan, *Carbohyd. Polym*., **207**, 108 (2019), https://doi.org/10.1088/2053-1591/ab22d9

[2] A. Vinod, R. Vijay, D. L. Singaravelu, M. R. Sanjay, S. Siengchin *et al*., *Mater. Res. Express*, **6**, 085406 (2019), https://doi.org/10.1088/2053-1591/ab22d9

[3] A. Vinod, R. Vijay and D. L. Singaravelu, *J. Nat. Fibers*, **15**, 648 (2018), https://doi.org/10.1080/15440478.2017.1354740
[4] S. Jothibasu, S. Mohanamurugan, R. Vijay, D. Lenin Singaravelu, A. Vinod *et al*., *J. Ind. Text.* **49**, 1036 (2020), https://doi.org/10.1177/1528083718804207
[5] R. Vijay, D. Lenin Singaravelu, A. Vinod, M. R. Sanjay, S. Siengchin *et al*., *Int. J. Biol. Macromol*., **125**, 99 (2019), https://doi.org/10.1016/j.ijbiomac.2018.12.056
[6] V. Chaudhary, P. K. Bajpai and S. Maheshwari, *J. Nat. Fibers*, **17**, 84 (2020), https://doi.org/10.1080/15440478.2018.1469451
[7] P. Manimaran, M. R. Sanjay, P. Senthamaraikannan, B. Yogesha, C. Barile *et al*., *J. Nat. Fibers*, **17**, 359 (2020), https://doi.org/10.1080/15440478.2018.1492491
[8] M. Sanjay and B. Yogesha, *Mater. Today Proc*., **4**, 2739 (2017), https://doi.org/10.1016/j.matpr.2017.02.151
[9] K. Ganesan, C. Kailasanathan, M. R. Sanjay, P. Senthamaraikannan and S. S. Saravanakumar, *J. Nat. Fibers*, **17**, 482 (2020), https://doi.org/10.1080/15440478.2018.1500340
[10] P. Manimaran, P. Senthamaraikannan, K. Murugananthan and M. R. Sanjay, *J. Nat. Fibers*, **15**, 29 (2018), https://doi.org/10.1080/15440478.2017.1302388
[11] A. Karakoti, S. Biswas, J. R. Aseer, N. Sindhu and M. R. Sanjay, *J. Nat. Fibers*, **17**, 189 (2020), https://doi.org/10.1080/15440478.2018.1477085
[12] P. Manimaran, M. R. Sanjay, P. Senthamaraikannan, M. Jawaid, S. S. Saravanakumar *et al*., *J. Nat. Fibers*, **16**, 768 (2019), https://doi.org/10.1080/15440478.2018.1434851
[13] R. Kumar, N. R. J. Hynes, P. Senthamaraikannan, S. Saravanakumar and M. R. Sanjay, *J. Nat. Fibers*, **15**, 822 (2018), https://doi.org/10.1080/15440478.2017.1369208
[14] P. Madhu, M. R. Sanjay, P. Senthamaraikannan, S. Pradeep, S. Siengchin *et al*., *J. Nat. Fibers*, **17**, 833 (2020), https://doi.org/10.1080/15440478.2018.1534191
[15] K. O. Reddy, K. R. N. Reddy, J. Zhang and A. Varada Rajulu, *J. Nat. Fibers*, **10**, 282 (2013), https://doi.org/10.1080/15440478.2013.800812
[16] M. Henriksson, G. Henriksson, L. Berglund and T. Lindström, *Eur. Polym. J.*, **43**, 3434 (2007), https://doi.org/10.1016/j.eurpolymj.2007.05.038
[17] N. A. M. Razali, R. Mohd Sohaimi, R. N. I. R. Othman, N. Abdullah, S. Z. N. Demon *et al*., *Polymers*, **14**, 387 (2022), https://doi.org/10.3390/polym14030387
[18] Q. Cheng, S. Wang and Q. Han, *J. Appl. Polym. Sci*., 115, 2756 (2010), https://doi.org/10.1002/app.30160
[19] M. Moniruzzaman and T. Ono, *Bioresour. Technol*., **127**, 132 (2013), https://doi.org/10.1016/j.biortech.2012.09.113
[20] M. M. Yashim, M. Mohammad, N. Asim, A. Fudholi and N. H. A. Kadir, *IOP Conf. Ser. Mater. Sci. Eng*., **1176**, 012004 (2021), https://doi.org/10.1088/1757-899X/1176/1/012004
[21] N. Rehman, S. Alam, I. Mian and H. Ullah, *Bull. Chem. Soc. Ethiop*., **33**, 61 (2019), https://doi.org/10.4314/bcse.v33i1
[22] S. S. M. Sukri, R. A. Rahman and H. Yaakob, *Romanian Biotechnol. Lett*., **19**, 13 (2014)
[23] Y. Chen, M. A. Stevens, Y. Zhu, J. Holmes and H. Xu, *Biotechnol. Biofuels*, **6**, 8 (2013), https://doi.org/10.1186/1754-6834-6-8
[24] U. Qasim, Z. Ali, M. S. Nazir, S. Ul Hassan, S. Rafiq *et al*., *Adv. Polym. Technol*., **2020**, e9765950 (2020), https://doi.org/10.1155/2020/9765950
[25] E. Damilano, F. Santos, B. Alencar, A. L. Reis, R. Souza *et al*., *Biomass Convers. Biorefin*., **8**, (2018), https://doi.org/10.1007/s13399-017-0277-3
[26] E. Abraham, B. Deepa, L. A. Pothan, M. Jacob, S. Thomas *et al*., *Carbohyd. Polym*., **86**, 1468 (2011), https://doi.org/10.1016/j.carbpol.2011.06.034
[27] J. K. Kim and I.-H. Kim, *J. Appl. Polym. Sci*., **79**, 2251 (2001), https://doi.org/10.1002/1097-4628(20010321)79
[28] P. B. Smith, A. J. Pasztor, M. L. McKelvy, D. M. Meunier, S. W. Froelicher *et al*., *Anal. Chem*., **69**, 95 (1997), https://doi.org/10.1021/a19700020
[29] M. D. Stelescu, A. Airinei, A. Bargan, N. Fifere, M. Georgescu *et al*., *Materials*, **15**, 6838 (2022), https://doi.org/10.3390/ma15196838
[30] G. Koronis, A. Silva and M. Fontul, *Compos. Part B Eng*., **44**, 120 (2013), https://doi.org/10.1016/j.compositesb.2012.07.004
[31] N. C. Loureiro, and J. L. Esteves, in "Green Composites for Automotive Applications", edited by G. Koronis and A. Silva, Woodhead Publishing, 2019, pp. 81–97, https://doi.org/10.1016/B978-0-08-102177-4.00004-5
[32] E. Sassoni, S. Manzi, A. Motori, M. Montecchi and M. Canti, *Energ. Build*., **77**, 219 (2014), https://doi.org/10.1016/j.enbuild.2014.03.033
[33] M. M. Davoodi, S. M. Sapuan, D. Ahmad, A. Aidy, A. Khalina *et al*., *Mater. Des*., **32**, 4857 (2011), https://doi.org/10.1016/j.matdes.2011.06.011
[34] S. D. S. Kopparthy and A. N. Netravali, *Compos. Part C*, **6**, 100169 (2021), https://doi.org/10.1016/j.jcomc.2021.100169
[35] N. M. Nurazzi, M. R. M. Asyraf, A. Khalina, N. Abdullah, H. A. Aisyah *et al*., *Polymers*, **13**, 646 (2021), https://doi.org/10.3390/polym13040646
[36] M. Jawaid and M. Thariq, "Sustainable Composites for Aerospace Applications", Woodhead Publishing, 2018
[37] L. E. Wise, M. Murphy and A. A. d'Addieco, *Paper Trade J*., **122**, 35 (1946)

[38] A. E. O. B. Sghaier, Y. Chaabouni, S. Msahli and F. Sakli, *Ind. Crop. Prod.*, **36**, 257 (2012), https://doi.org/10.1016/j.indcrop.2011.09.012
[39] K. O. Reddy, C. U. Maheswari, M. S. Dhlamini, B. M. Mothudi, V. P. Kommula *et al.*, *Carbohyd. Polym.*, **188**, 85 (2018), https://doi.org/10.1016/j.carbpol.2018.01.110
[40] S. Naduparambath and E. Purushothaman, *Cellulose*, **23**, 1803 (2016), https://doi.org/10.1007/s10570-016-0904-3
[41] N. El Miri, K. Abdelouahdi, A. Barakat, M. Zahouily, A. Fihri *et al.*, *Carbohyd. Polym.*, **129**, 156 (2015), https://doi.org/10.1016/j.carbpol.2015.04.051
[42] D. Trache, A. Donnot, K. Khimeche, R. Benelmir and N. Brosse, *Carbohyd. Polym.*, **104**, 223 (2014), https://doi.org/10.1016/j.carbpol.2014.01.058
[43] R. A. Ilyas, S. M. Sapuan and M. R. Ishak, *Carbohyd. Polym.*, **181**, 1038 (2018), https://doi.org/10.1016/j.carbpol.2017.11.045
[44] P. Penjumras, R. B. A. Rahman, R. A. Talib and K. Abdan, *Agric. Agric. Sci. Proc.*, **2**, 237 (2014), https://doi.org/10.1016/j.aaspro.2014.11.034
[45] L. Y. Xiang, M. A. P. Mohammed and A. Samsu Baharuddin, *Carbohyd. Polym.*, **148**, 11 (2016), https://doi.org/10.1016/j.carbpol.2016.04.055
[46] M. Choi, Y.-R. Kang, I.-S. Lim and Y. H. Chang, *Prev. Nutr. Food Sci.*, **23**, 166 (2018), https://doi.org/10.3746/pnf.2018.23.2.166
[47] M. F. Rosa, E. S. Medeiros, J. A. Malmonge, K. S. Gregorski, D. F. Wood *et al.*, *Carbohyd. Polym.*, **81**, 83 (2010), https://doi.org/10.1016/j.carbpol.2010.01.059
[48] M. Poletto, V. Pistor, M. Zeni and A. J. Zattera, *Polym. Degrad. Stab.*, **96**, 679 (2011), https://doi.org/10.1016/j.polymdegradstab.2010.12.007
[49] F. Xu, J. Yu, T. Tesso, F. Dowell and D. Wang, *Appl. Energ.*, **104**, 801 (2013), https://doi.org/10.1016/j.apenergy.2012.12.019
[50] K. Fackler, J. S. Stevanic, T. Ters, B. Hinterstoisser, M. Schwanninger *et al.*, *Holzforschung*, **65**, 411 (2011), https://doi.org/10.1515/hf.2011.048
[51] M. Poletto, H. L. Ornaghi and A. J. Zattera, *Materials*, **7**, 6105 (2014), https://doi.org/10.3390/ma7096105
[52] K. O. Reddy, C. U. Maheswari, M. Shukla and A. V. Rajulu, *Mater. Lett.*, **67**, 35 (2012), https://doi.org/10.1016/j.matlet.2011.09.027
[53] L. Chen, J. Y. Zhu, C. Baez, P. Kitin and T. Elder, *Green Chem.*, **18**, 3835 (2016), https://doi.org/10.1039/C6GC00687F
[54] C. P. Azubuike and A. O. Okhamafe, *Int. J. Recycl. Org. Waste Agric.*, **1**, 9 (2012), https://doi.org/10.1186/2251-7715-1-9
[55] C.-F. Liu, J.-L. Ren, F. Xu, J.-J. Liu, J.-X. Sun and R.-C. Sun, *J. Agric. Food Chem.*, **54**, 5742 (2006), https://doi.org/10.1021/jf060929o
[56] H. Yang, R. Yan, H. Chen, D. H. Lee and C. Zheng, *Fuel*, **86**, 1781 (2007), https://doi.org/10.1016/j.fuel.2006.12.013
[57] J. Lamaming, R. Hashim, O. Sulaiman, C. P. Leh, T. Sugimoto *et al.*, *Carbohyd. Polym.*, **127**, 202 (2015), https://doi.org/10.1016/j.carbpol.2015.03.043
[58] I. Y. A. Fatah, H. P. S. A. Khalil, M. S. Hossain, A. A. Aziz, Y. Davoudpour *et al.*, *Polymers*, **6**, 2611 (2014), https://doi.org/10.3390/polym6102611
[59] K. O. Reddy, C. U. Maheswari, D. J. P. Reddy and A. V. Rajulu, *Mater. Lett.*, **63**, 2390 (2009), https://doi.org/10.1016/j.matlet.2009.08.035
[60] N. Johar, I. Ahmad and A. Dufresne, *Ind. Crop. Prod.*, **37**, 93 (2012), https://doi.org/10.1016/j.indcrop.2011.12.016
[61] M. J. M. Ridzuan, M. S. Abdul Majid, A. Khasri, K. S. Basaruddin and A. G. Gibson, *Compos. Part B Eng.*, **160**, 84 (2019), https://doi.org/10.1016/j.compositesb.2018.10.029
[62] M. J. M. Ridzuan, M. S. A. Majid, A. Khasri, E. H. D. Gan, Z. M. Razlan *et al.*, *J. Mater. Res. Technol.*, **8**, 5384 (2019), https://doi.org/10.1016/j.jmrt.2019.09.005
[63] O. Somseemee, P. Sae-Oui and C. Siriwong, *Ind. Crop. Prod.*, **171**, 113881 (2021), https://doi.org/10.1016/j.indcrop.2021.113881
[64] Y. Liu, A. Liu, S. A. Ibrahim, H. Yang and W. Huang, *Int. J. Biol. Macromol.*, **111**, 717 (2018), https://doi.org/10.1016/j.ijbiomac.2018.01.098
[65] S. K. Chakraborty, D. K. Setua and S. K. De, *Rubber Chem. Technol.*, **55**, 1286 (1982), https://doi.org/10.5254/1.3535930
[66] G. R. Hamed, *Rubber Chem. Technol.*, **73**, 524 (2000), https://doi.org/10.5254/1.3547603
[67] J. Kruželák, R. Sýkora and I. Hudec, *Chem. Pap.*, **70**, 1533 (2016), https://doi.org/10.1515/chempap-2016-0093
[68] Ł. Zedler, X. Colom, J. Cañavate, M. R. Saeb, J. T. Haponiuk *et al.*, *Polymers*, **12**, 545 (2020), https://doi.org/10.3390/polym12030545
[69] J. Wang, S. Pan, Y. Zhang and S. Guo, *Polym. Test.*, **59**, 253 (2017), https://doi.org/10.1016/j.polymertesting.2016.12.034
[70] M. J. M. Ridzuan, M. S. A. Majid, M. Afendi, S. N. Aqmariah Kanafiah, J. M. Zahri *et al.*, *Mater. Des.*, **89**, 839 (2016), https://doi.org/10.1016/j.matdes.2015.10.052
[71] B. W. Chieng, S. H. Lee, N. A. Ibrahim, Y. Y. Then and Y. Y. Loo, *Polymers*, **9**, 355 (2017), https://doi.org/10.3390/polym9080355
[72] J. Kruželák, K. Hloženková, A. Kvasničáková, K. Tomanová and I. Hudec, *Polymers*, **14**, 1921 (2022), https://doi.org/10.3390/polym14091921
[73] C. Sareena, M. Sreejith, M. Ramesan and E. Purushothaman, *J. Reinf. Plast. Compos.*, **33**, 412 (2014), https://doi.org/10.1177/0731684413515954